Journal of Membrane Science 514 (2016) 250–263

Contents lists available at ScienceDirect

Journal of Membrane Science

journal homepage: www.elsevier.com/locate/memsci

Understanding the non-solvent induced phase separation (NIPS) effect during the fabrication of microporous PVDF membranes *via* thermally induced phase separation (TIPS)

Jun Tae Jung [a,1], Jeong F. Kim [a,1], Ho Hyun Wang [a], Emanuele di Nicolo [b], Enrico Drioli [a,c,*], Young Moo Lee [a,*]

[a] Department of Energy Engineering, Hanyang University, Republic of Korea
[b] Solvay Specialty Polymers, R&D Center, Bollate, Italy
[c] Institute on Membrane Technology (ITM-CNR), Via P. Bucci 17/C, 1-87030 Rende, CS, Italy

ARTICLE INFO

Article history:
Received 19 March 2016
Received in revised form
28 April 2016
Accepted 29 April 2016
Available online 9 May 2016

Keywords:
Non-solvent induced phase separation (NIPS)
Green solvent
PVDF
Thermally induced phase separation (TIPS)

ABSTRACT

The thermally induced phase separation (TIPS) method is regaining momentum as a competitive platform to fabricate highly porous microporous membranes. In membrane technology, there has been an active search for more sustainable ways to fabricate polymeric membranes using green solvents. Rhodiasolv PolarClean® is a recently identified environmentally friendly TIPS solvent that shows high potential for the preparation of microporous PVDF membranes. Interestingly, its high miscibility with water induces a nonsolvent-induced phase separation (NIPS) effect on the membrane surface and this simultaneous NIPS-TIPS effect is referred to as the combined NIPS-TIPS (N-TIPS) method. In this work, a thorough investigation was carried out to understand the underlying phenomena in the membrane formation kinetics during the N-TIPS process. It was found that the NIPS and TIPS morphology can be tailored to control the mechanical properties, pore size distribution, and flux of the prepared membranes. For instance, increasing the coagulation bath solvent concentration facilitated the formation of a spherulitic morphology, whereas increasing the bath temperature induced the formation of a bicontinuous morphology free of macrovoids. It was determined that by controlling the phase separation kinetics, the mechanical properties of the prepared PVDF membranes could be remarkably improved from 0.9 MPa to 6.1 MPa. Several pore-forming additives including polyvinylpyrrolidone, Pluronics F-127, LiCl, and glycerol were employed to induce surface pores and their effects were thoroughly characterized. The membranes prepared with Pluronic additives exhibited high water permeabilities up to 2800 L m^{-2} h^{-1} bar^{-1} with narrow pore size distributions.

1. Introduction

As the $32 billion membrane market continuously advances in terms of membrane fabrication and process systems, polymeric membranes steadily hold the dominant position in most of application fields. Among the available polymeric membranes, poly (vinylidene fluoride) (PVDF) provides outstanding performances based on its excellent inherent properties such as high thermal stability, great chemical resistance, and good processability [1].

The market share for MF and UF membranes is nearly half of the membrane market [2] with a wide application spectrum covering food and dairy industries, wastewater treatment, hemodialysis, and RO pretreatment [3,4]. MF and UF are pressure-driven processes where the morphology of the membrane plays a critical role in determining the final performance (flux and selectivity). Generally, hydrophilic membranes with a high porosity, strong mechanical properties, and narrow pore size distribution are preferred. More recently, however, hydrophobic membranes are becoming important for new emerging applications such as membrane distillation (MD) and membrane crystallization (MCr) [5,6]. Notably, PVDF is intrinsically hydrophobic and hence, it is one of the promising candidates for contactor applications [7]. Rationally, controlling the membrane morphology with respect to the desired application is the key factor in developing successful membranes [8].

Polymeric membranes can be fabricated via several routes and the phase inversion method is currently the mainstream technique used for most membrane applications. Among the different phase inversion methods, two techniques are frequently used:

* Corresponding authors at: Department of Energy Engineering, Hanyang University, Republic of Korea.
E-mail addresses: e.drioli@itm.cnr.it (E. Drioli), ymlee@hanyang.ac.kr (Y.M. Lee).
[1] Authors contributed equally.

http://dx.doi.org/10.1016/j.memsci.2016.04.069
0376-7388/

nonsolvent induced phase separation (NIPS) and thermally induced phase separation (TIPS). The NIPS method has three components (polymer, solvent, and nonsolvent) and membranes are fabricated by controlling the interaction between the polymer and solvent(s) of interest. The membranes prepared by NIPS typically show a dense surface with an asymmetric morphology, suitable for RO and NF processes [9]. On the other hand, the TIPS method is typically employed with semi-crystalline polymers and the main driving force is induced by removing the thermal energy from the dope solution [10]. The membranes prepared via the TIPS method exhibit a highly porous and symmetric structure which is suitable for MF and membrane contactor applications [11]. Notably, as the TIPS method is composed of only two components (polymer and solvent), membranes fabricated by the TIPS method are inherently more reproducible and less prone to defects [12]. In addition, the elevated working temperatures in the TIPS method allow a wider selection of solvents and polymers, albeit with higher energy consumption [12].

One of the pressing challenges faced in membrane technology is the high toxicity of the solvents used during membrane fabrication. For instance, common NIPS solvents such as NMP (*N*-Methyl-2-pyrrolidone) and DMF (*N,N*-dimethyl formamide) [13,14] have encountered increasing regulations due to concerns over potential health issues [15]. Similarly, DEP (diethyl phthalate), DBP (dibutyl phthalate), and DOP (dioctyl phthalate), which are common phthalate-based TIPS solvents, are also drawing concerns from industries due to their bioaccumulation tendency and high toxicity [16]. DBP, in particular, was found to damage human organs and has been banned by U.S. federal regulations for use in cosmetics and childcare products [17].

As a result of the environmental concerns, there have been many active research efforts to replace toxic solvents with environmentally friendly alternatives. Cha et al. employed γ-butyrolactone (GBL) in a modified TIPS process for the preparation of MF membranes [18] and Rajabzadeh et al. evaluated glycerol triacetate (triacetin) as a new TIPS solvent [19,20]. Sawada et al. and Kim et al. carried out thorough analyses of the effects of citrate-based non-toxic solvents (*e.g.* Citroflex A4) in PVDF membrane preparation via the TIPS process [21,22]. Cui et al. also identified a new environmentally benign solvent, TEGDA (triethylene glycol diacetate), which induced an interesting fibrillar morphology [23].

As mentioned above, these new green solvents can only dissolve the polymer of interest (*i.e.* PVDF) at elevated temperatures. Hence, upon casting the membrane at a high temperature, the crystallization temperature (T_C) and cooling rate of the cast membranes are the key parameters which determine the final membrane morphology [24]. However, if there is reasonable affinity between the solvent and coagulation medium, the coagulation medium itself can be another parameter in membrane preparation, as it is in the NIPS process [25]. For example, when water, a common coagulation medium, is employed for cooling the cast membrane, the water and solvent could diffuse into each other affecting the phase separation. Therefore, when a water-soluble TIPS solvent is used, both the NIPS and TIPS effects can co-exist. Such phenomenon is referred to as the combined NIPS and TIPS (N-TIPS) method [12] and has been gaining interest as an attractive candidate for controlling the morphology and performance [12]. For instance, combining the advantages of NIPS and TIPS could yield highly permeable membranes with strong mechanical properties [12]. Since Matsuyama et al. first pioneered the N-TIPS method in 2002 [26], there have been many studies to understand this new emerging method by employing a co-solvent [27] or by controlling the system temperature [28]. However, due to its complexity, fabricating membranes with desired structures and performances have not been fully elucidated.

Recently, Hassankiadeh et al. conducted studies using a water-soluble green solvent called PolarClean® (methyl-5-(dimethylamino)-2-methyl-5-oxopentanoate) and interestingly, both NIPS and TIPS morphologies were observed [29]. PolarClean® is an ecofriendly biodegradable solvent with no reported health hazards [29]. In addition, it has a high boiling point (280 °C) with a low vapor pressure, meeting the basic requirements for a TIPS solvent. However, due to the high affinity of PolarClean® towards water, a dense outer layer was observed on the prepared membranes and hence, different pore-forming additives were employed to induce surface pores. However, the study was limited to high polymer concentrations (above 30 wt%) without conducting a detailed analysis to understand the detailed correlation between the NIPS and TIPS effects on the membrane performance.

In solution thermodynamics, the interaction between a semi-crystalline polymer and solvent determines the binodal and crystallization curves [30]. In addition, since the binodal and crystallization curves are also affected by the temperature and non-solvent, it is well accepted that both curves are functions of temperature and the interactions between the polymer, solvent, and nonsolvent [31]. Therefore, it is necessary to fully understand the formation of the phase diagram to interpret the resulting NIPS and TIPS effects.

In general, three-dimensional binodal surfaces of a certain polymer/solvent/nonsolvent system at different temperature can be represented as shown in Fig. 1a. If the polymer has a semi-crystalline property, the crystallization should be taken into account (Fig. 1b). When Fig. 1b is projected into the Temp-Polymer plane (Plane 1), a typical TIPS phase diagram can be obtained, as shown in Fig. 1c. On the other hand, when Fig. 1b is projected into Plane 2 (at a fixed temperature), a typical NIPS phase diagram is obtained (Fig. 1d).

As discussed previously, the location and size of the binodal curve is a strong function of polymer-solvent-nonsolvent interaction. If the polymer-solvent interaction is poor, *i.e.* bad solvent, the size of the binodal curve expands outward, as shown in Fig. 1e. Naturally, when Fig. 1e is projected into the Temp-Polymer plane (Plane 3), another typical TIPS phase diagram can be obtained with a distinct binodal line (Fig. 1f). On the other hand, if the interaction between the polymer and solvent is strong, *i.e.* good solvent, the size of the binodal is relatively small and an L-L separation region is not observed in the TIPS plane (plane 1 and 3), which is the case with the PVDF/NMP system [3].

It is important to note that phase diagrams only represent the system thermodynamics and it is crucial to take kinetic aspects into account when analyzing the membrane formation mechanism [32,33]. For example, the driving force for phase separation in the TIPS process primarily results from the decrease of the polymer solubility in a solvent as the temperature is lowered at a controlled rate [34]. Therefore, the cooling rate has a dominant influence on the final membrane morphology. Indeed, most TIPS solvents usually have poor interactions with the polymer and follow the phase diagrams shown in Fig. 1e and f. In such cases, the dope composition and cooling kinetic determines whether the system will undergo liquid-liquid separation (L-L separation) or simultaneous solid-liquid (S-L)/liquid-liquid separations [12]. On the other hand, if the TIPS solvent has a good interaction with the polymer, *i.e.* good solvent, the crystallization rate at a certain temperature becomes significantly slow or even disappears at a lower polymer concentration (Fig. 1c). In this case, a nonsolvent is required to induce crystallization, as shown in Fig. 1d. Therefore, the solvent-nonsolvent diffusion kinetics as well as the cooling rate should be carefully controlled [31].

In this study, we investigated the N-TIPS phenomena in the PolarClean®/PVDF system in detail to fundamentally understand the competitive behavior of NIPS and TIPS during the membrane formation process. In addition, we optimized the membrane

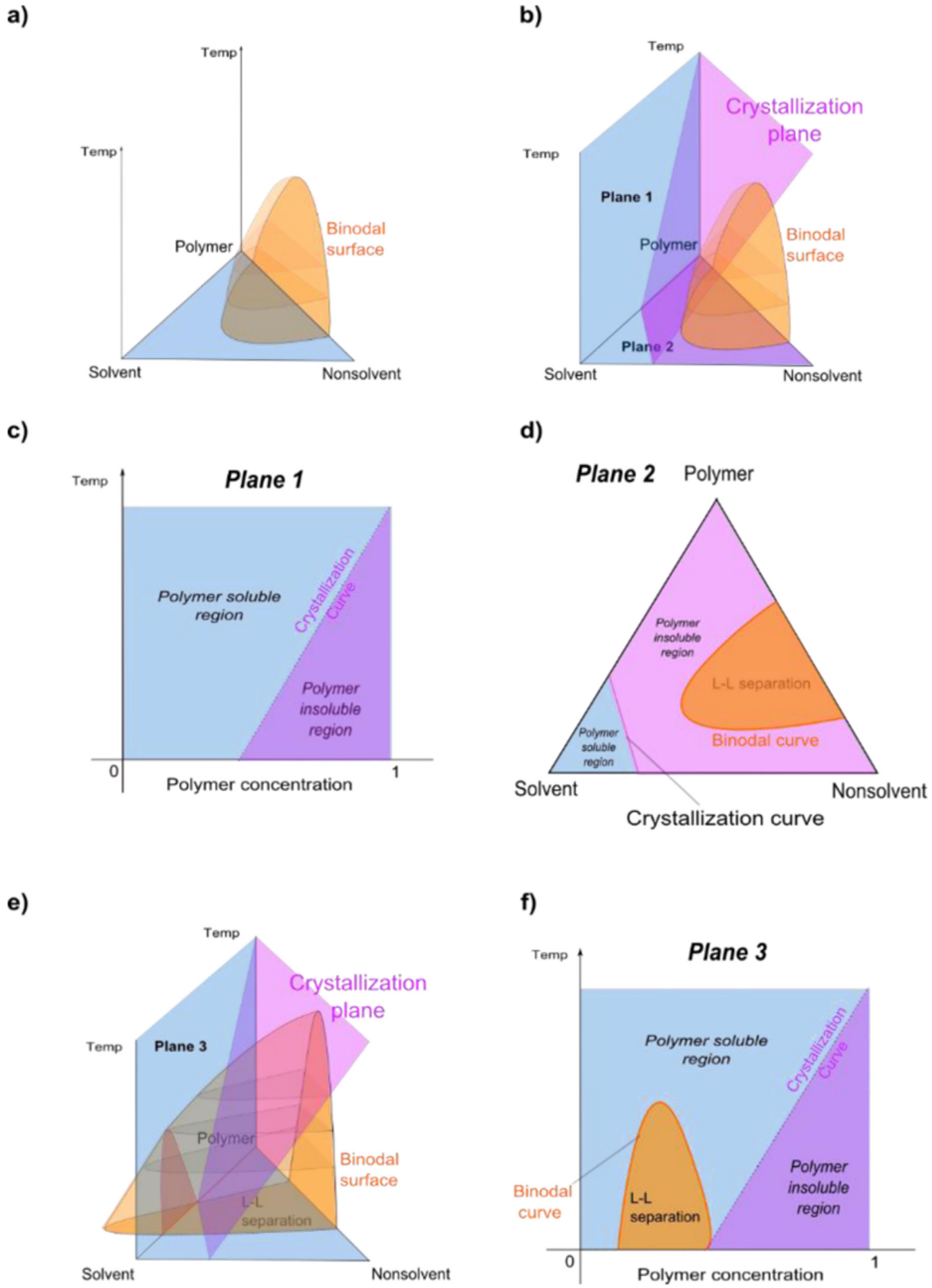

Fig. 1. 2-D and 3-D phase diagram illustrations of hypothetical polymer-solvent systems: (a) 3-D phase diagram at different temperatures, (b) 3-D phase diagram with a semi-crystalline polymer and a *good* solvent, (c) a 2-D binary phase diagram of a polymer and a *good* solvent system, (d) a 2-D ternary phase diagram of a polymer and a *good* solvent system, (e) 3-D phase diagram with a semi-crystalline polymer and a *bad* solvent at different temperatures, and (f) a 2-D binary phase diagram of a polymer and a *bad* solvent system.

performance by controlling the two effects in tandem with independent parameters such as the dope composition, coagulation bath composition, and bath temperature. The effects of each parameter on the membrane morphology (and respective mechanical properties), water permeability, and porosity were analyzed in detail.

2. Experimental

2.1. Materials

PVDF (Solef® 1015) and Rhodiasolv PolarClean® (Methyl-5-(dimethylamino)-2-methyl-5-oxopentanoate) were kindly provided by Solvay Specialty Polymers (Bollate, Italy). Pluronic F-127, LiCl, glycerol, and polyvinylpyrrolidone (PVP, Mw = 10 kDa) were purchased from Sigma-Aldrich. Analytical grade ethanol (EtOH) and hexane were purchased from Daejung Chemicals (Siheung, South Korea).

2.2. Determination of the binary phase diagram

The crystallization temperatures of the PVDF/PolarClean® system were determined using a differential scanning calorimeter (DSC Q20, TA Instruments, New Castle, DE, USA). Homogeneous PVDF/PolarClean® solutions were prepared under different concentrations and then placed in tared sample pans (Tzero Hermetic pan, TA Instruments). Each sample was heated at a rate of 10 °C per minute to 200 °C and then held for 10 min to exclude any thermal history of the sample. The sample was then cooled at a rate of 1 °C per minute to −50 °C. The crystallization temperature was determined to occur at the maximum exothermic peak. To determine the degree of crystallinity of membranes, the first DSC melting point peak was integrated and compared to the theoretical melting enthalpy of PVDF (104.5 J g^{-1}).

2.3. Preparation of flat sheet membranes

The general preparation method is described below. A dope solution of a known concentration (15–30 wt% polymer) was prepared by mixing the PVDF powder and PolarClean® (sonicated) at 140 °C until the solution became homogeneous. For the membranes prepared with additives, 5 or 10 wt% of either PVP10k or Pluronic F-127, or LiCl (0.5 wt%)+Glycerol (4 wt%) was added to the dope solution. The homogeneous dope solution was degassed for 1 h and then cast onto a glass plate using a casting knife (Elcometer *Ltd.*, Manchester, UK) set at a thickness of 200 μm. The cast membrane was subsequently immersed into a coagulation bath. The composition and temperature of the coagulation bath were varied to study their effects. The tested compositions of the coagulation bath were water and PolarClean®:water (*vol:vol*) ratios of 2:6, 4:6, and 6:4. The tested temperatures were 5, 20, 40, and 60 °C. The membranes were kept in the coagulation bath for 30 min and then washed in a washing bath (water, 20 ± 3 °C) overnight. Then, the membranes were washed with EtOH three times to extract any remaining solvents, washed with hexane three times to remove residual EtOH, and then dried from hexane to preserve the pores.

2.4. Characterization of the prepared membranes

The microscopic morphologies of the membranes were observed using a scanning electron microscope (FE-SEM S-4800, Hitachi, Tokyo, Japan) at 10–15 kV. The membranes were sampled in liquid nitrogen and then sputtered with platinum for 90 s at 15 mA using a platinum sputter (E-1045, Hitachi).

The overall porosity of the membrane was calculated using the following equation:

$$\varepsilon = 1 - \frac{M_p/\rho_p}{w \times l \times t} \quad (1)$$

where Mp and ρ_p represent the polymer mass and density (1.75 g cm^{-3}), respectively, and w, *l*, and t are the width, length, and thickness of the prepared membranes, respectively.

The mechanical properties of the prepared membranes were measured using a universal testing machine (AGS-J 500N, Shimadzu, Kyoto, Japan). The sample gauge length was 20 mm and the elongation rate was 10 mm min^{-1}.

Water permeation tests were performed by first wetting the membranes with EtOH for at least 30 min to open the permeation pathway. They were then placed in a water permeation cell with an effective surface area of 6.23 cm^2 (Sepratek Ltd., Daejeon, South Korea) and pressurized with N_2 to 0.5 bar. The water flux was measured every 30 min until three consecutive values converged (approximately 5 h). A significant flux decline was observed in the beginning due to compaction. The pore size distributions of the membranes were analyzed using ImageJ software.

3. Results and discussion

3.1. Phase diagram of the PVDF/PolarClean® system

Understanding the solution thermodynamics of a polymer/solvent system using a phase diagram is very important to explain the observed phase separation phenomena. Phase diagrams can reflect thermodynamic properties such as the mutual affinity between a polymer and solvent, which is an essential parameter in membrane fabrication via phase inversion. In the PVDF/PolarClean® system, PolarClean® cannot solvate PVDF at ambient temperature and hence, a high temperature environment is required to use PolarClean® for PVDF membrane fabrication via TIPS. As discussed in the Introduction section, a TIPS system is usually described using a binary phase diagram since the parameters that can affect the phase separation are the polymer content and the temperature of the system, as shown in Fig. 2 for the PVDF/PolarClean® system.

The solid line in Fig. 2 represents the crystallization temperatures of the corresponding polymer concentration and the dotted line shows the estimated (extrapolated) crystallization temperatures. As illustrated in Fig. 2, neither a cloud point nor distinct crystallization temperature was detected below 25 wt% polymer from the DSC data, which implies that the compatibility between PVDF and PolarClean® is very high, slowing down the crystallization kinetics.

To investigate this phenomenon further, 20 wt% dope solutions (in PolarClean®) were prepared and placed under different temperatures (60 °C, 40 °C, 20 °C, 5 °C, and −20 °C, see Supporting information). The prepared solutions were checked every 8 h for

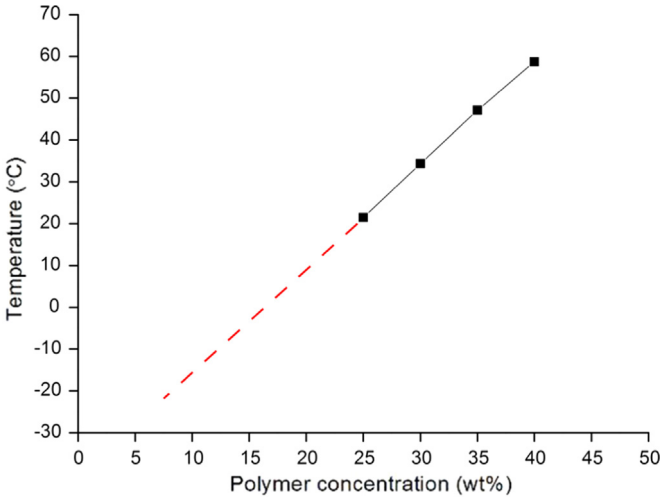

Fig. 2. Phase diagram of the PVDF/ PolarClean® system. The crystallization points were determined by DSC.

Table 1
Hansen solubility parameter and Ra values of the solvent and nonsolvent for PVDF.

		δ_d	δ_p	δ_h	Ra ($MPa^{0.5}$)	Ref.
Polymer	PVDF	17.2	12.5	9.2	–	[39]
TIPS solvents	Polarclean®	15.8	10.7	9.2	3.3	
	Dibutyl phthalate (DBP)	17.8	8.6	4.1	6.5	[40]
	Triethylene glycol diacetate (TEGDA)	16.4	2.1	9.8	10.5	[23]
	Acetyl tributyl citrate (ATBC)	16.02	2.56	8.55	10.2	[22]
NIPS solvents	N-methyl-2-pyrrolidone (NMP)	18	12.3	7.2	2.6	[35]
	N,N-dimethylformamide (DMF)	17.4	13.7	11.3	2.5	[35]
	Dimethylsulfoxide (DMSO)	18.4	16.4	10.2	4.7	[35]
Nonsolvents	Water	15.6	16	42.3	33.4	[39]
	Ethanol	15.8	8.8	19.4	11.2	[35]

any visible phase separation. Even after 24 h, all of the solutions remained in the solution state without any visible phase separation or crystallization. This observation is very similar to that of homogeneous PVDF/NMP and PVDF/DMF systems [30,35,36]. After 4 days, the solutions prepared at 20 °C, 5 °C, and −20 °C became partially opaque, indicating that crystallization occurred.

The mutual affinity between a polymer and solvent can be estimated using the solubility parameter approach. The distance between the Hansen parameters in Hansen space (*Ra*) can describe the polymer-solvent compatibility [37,38], which can be calculated via the Hansen solubility parameters using Eq. (2), as listed in Table 1 [37].

$$Ra = \sqrt{4(\delta_{d1} - \delta_{d2})^2 + (\delta_{p1} - \delta_{p2})^2 + (\delta_{h1} - \delta_{h2})^2} \quad (2)$$

here, δ_d, δ_p, and δ_h represent the dispersion, polar, and hydrogen bond interactions, respectively.

A polymer-solvent system with a low Ra value is considered to have good compatibility and is likely to have a small binodal curve (wide solvation range). Therefore, a system with a low Ra value is likely to undergo solid-liquid separation at high polymer concentrations but no liquid-liquid separation (demixing) at low polymer concentrations due to the small binodal curve (see Fig. 1 in Section 1). It can be seen that the Ra value of the PVDF/PolarClean® system (3.3 $MPa^{0.5}$) is very close to that of PVDF/NMP (2.6 $MPa^{0.5}$)) and PVDF/DMF systems (2.5 $MPa^{0.5}$). Notably, the TIPS binary phase diagrams for both the PVDF/NMP and PVDF/DMF systems show neither a binodal curve nor a crystalline temperature below a polymer concentration of 25 wt%, indicating that the system is thermodynamically stable [30,36]. Therefore, the low Ra value calculated for the PVDF/PolarClean® system supports the missing binodal curve observed in Fig. 2. It also suggests that it is difficult to achieve membrane fabrication *via* the TIPS process alone in the PVDF/PolarClean® system, especially at low polymer contents (below 25 wt%).

Unlike typical TIPS solvents such as phthalate-based or citrate-based solvents [11,41,42], PolarClean® has a high miscibility with water. Hence, when the cast membranes from PVDF/PolarClean® are immersed into a coagulation water bath at 5 °C, not only polymer crystallization but also mutual diffusion between the solvent in the dope solution (PolarClean®) and the nonsolvent in the coagulation bath (water) occurs, yielding the NIPS-TIPS morphology, as shown in Fig. 3.

It can be seen that regardless of the initial polymer concentration, a dense surface and macrovoids are clearly observed on the upper part of the membrane, which is a common phenomenon in nonsolvent induced phase separation (NIPS). Also, higher fraction of macrovoids are observed with lower polymer concentration. On the other hand, a spherulitic TIPS morphology can be observed on the lower part of the membrane, particularly for high polymer content membranes (20–25 wt%). Accordingly, it can be deduced from Figs. 2 and 3 that the NIPS and TIPS effects show a competitive behavior depending on the membrane fabrication conditions. Hence, it is essential to also study the NIPS effect during a TIPS phase inversion process for the optimization of membrane morphology and performances, particularly when using a water-miscible solvent.

3.2. Morphological study of the solvent/nonsolvent diffusion rate in PVDF/PolarClean® membranes

A significant limitation of the phase diagram is that it only reflects the thermodynamic stability and neglects kinetic factors such as the solvent/nonsolvent diffusion rate and polymer crystallization rate, which are considered to be more important parameters in membrane fabrication [12]. Since the NIPS process is driven by the solvent/nonsolvent exchange, one of the effective ways to control the NIPS effect is to slow the exchange rate by changing the coagulation bath concentration [24]. Adding the system solvent (PolarClean®) in the coagulation bath decreases the concentration gradient which leads to a slower diffusion rate of PolarClean® from the dope into the coagulation bath and hence, the NIPS effect is expected to diminish. The SEM images of the membranes (15 wt% PVDF) prepared using different coagulation bath concentrations are shown in Fig. 4.

At a fixed polymer concentration (15 wt% PVDF), Fig. 4 illustrates the changes of the membrane morphology in different coagulant environments. As the driving force for the polymer crystallization (TIPS) remained the same (5 °C coagulation bath), the change of the membrane morphology was primarily due to the change of the NIPS effect. It can be seen that the NIPS morphology (macrovoids) is replaced by the TIPS morphology (spherulites) with increasing solvent concentration in the coagulation bath. This observation is due to the reduced mass exchange rate (slower solvent-nonsolvent transfer). In general, slower solvent-nonsolvent transfer induces delayed demixing and the resulting membranes show a dense skin and a bicontinuous support layer [43], accompanied by the suppression of macrovoids. [44] Interestingly, Fig. 4 shows that the macrovoids were suppressed but instead of the expected bicontinuous structure, spherulites were observed. This observed membrane morphology can be explained by kinetic factors during the membrane preparation.

First, the TIPS effect was maximized and the NIPS effect was minimized by keeping the coagulation bath temperature at 5 °C to slow down the mass diffusion rate. Minimizing the NIPS effect, by definition, leaves more time for TIPS (crystallization) to occur and an upward trend of crystallinity was observed, as shown in Fig. 5a. It can be seen that the crystallinity of the membrane increased from 57 to 69% as the PolarClean® fraction in the coagulation bath increased from 0 to 60 wt%. It should be noted that a PolarClean® fraction above 60 wt% was also attempted to completely remove the NIPS effect but no phase separation was observed. Notably, as shown in Fig. 4, all of the prepared membranes showed a dense skin layer on the top surface regardless of the coagulation bath concentration and low or no water permeability was observed at 1 bar (see Supporting information).

It has been widely reported in the literature that the presence of macrovoids weakens the mechanical properties of a membrane [43] and that the TIPS-prepared membranes show high mechanical strengths [45]. Since the prepared membranes exhibited both a macrovoid morphology and spherulitic morphology (TIPS), their

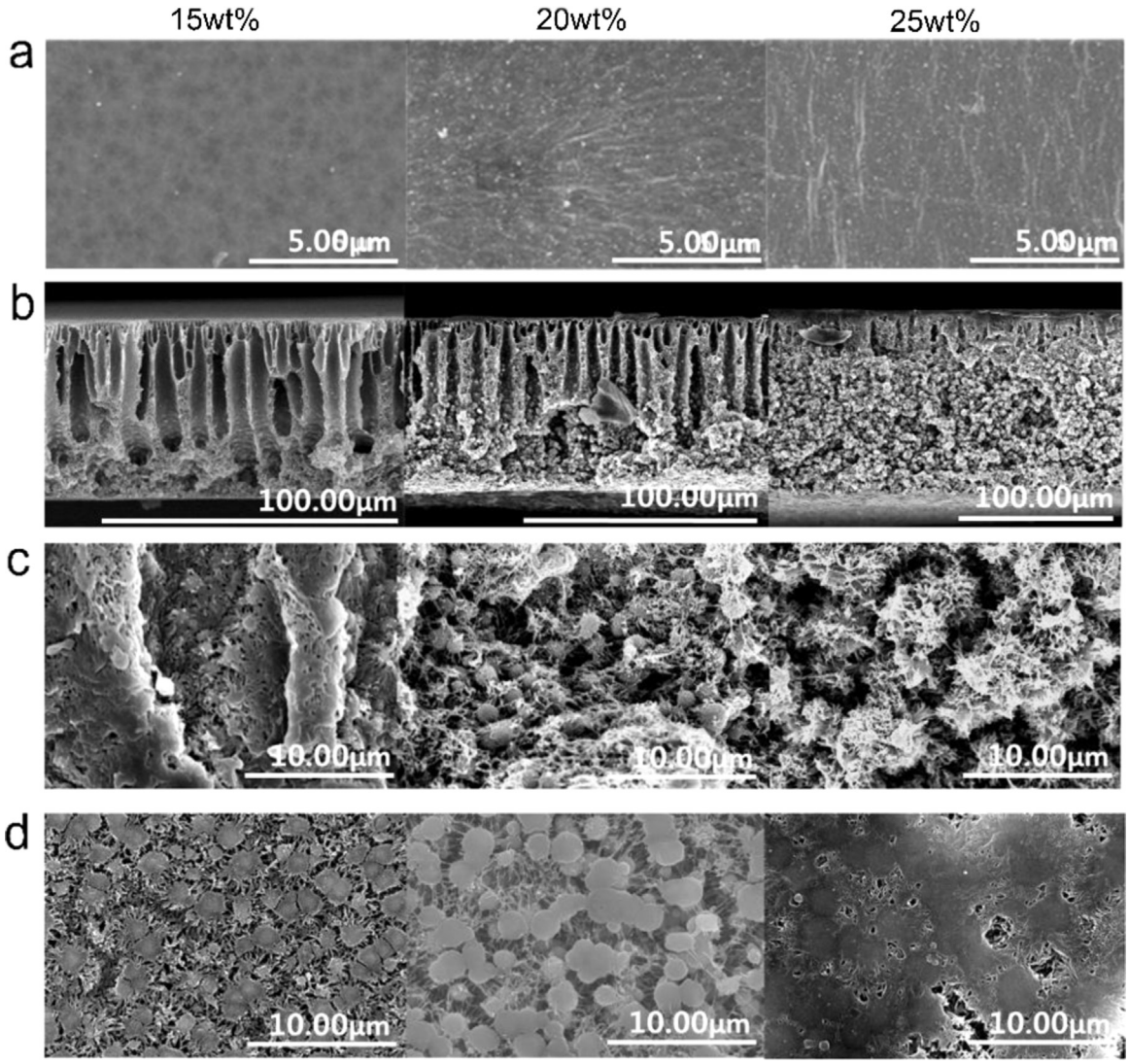

Fig. 3. SEM images illustrating the effect of the polymer concentration on PVDF/PolarClean® membranes: (a) top surface, (b) cross-section, (c) magnified cross-section, and (d) bottom surface. The bottom surface refers to the membrane surface that is in contact with the glass.

overall mechanical properties were measured as a function of the PolarClean® fraction, as shown in Fig. 5b.

Contrary to our expectation, the mechanical properties of the membranes decreased gradually with increasing TIPS morphology (*i.e.* decreasing macrovoids). As observed in Fig. 5b, both the tensile strength and elongation at break of the membranes decreased from 2.5 MPa to 0.9 MPa and 143 to 56%, respectively, with increasing PolarClean® content in the coagulation bath. Although these trends do not match what is reported in the literature, it can be explained from the phase separation mechanism perspective.

In a typical NIPS phase separation process, a homogeneous dope solution is exposed to an environment (coagulation bath) where the solution becomes thermodynamically unstable. The unstable solution then passes through a binodal curve where phase demixing occurs (*liquid-liquid phase separation*) into a polymer-rich and polymer-poor solution which eventually becomes the membrane matrix and pores, respectively [46]. The rate and extent of phase demixing determines the overall membrane structure and mechanical properties.

On the other hand, spherulites develop from *solid-liquid phase separation* via the nucleation-growth mechanism of polymer crystals [47] rather than passing through a binodal line. Hence, the spherulites grow independently from each other and they do not form an interconnected polymer-rich matrix found in *liquid-liquid phase separation*. Naturally, membranes with spherulitic structures (disconnected) are weaker than membranes with a bicontinuous (cellular) structure formed from *liquid-liquid phase separation* [48]. In addition, spherulites typically nucleate from a dope solution with a high polymer content, typically above 25 wt%, where polymer crystallization by thermal solubility becomes the major driving force for phase separation [10]. Hence, membranes with a spherulitic structure have been considered as strong membranes due to the high polymer concentration rather than the effects of spherulites. Therefore, an interesting conclusion can be deduced in which the spherulitic morphology results in mechanically fragile membranes, possibly worse than membranes with macrovoids. Hence, much of the recent TIPS research has focused on inducing a bicontinuous structure while minimizing spherulite formation [48,49].

It can also be seen in Fig. 5a that, as expected, the overall porosity of the membranes remained the same at $80.2 \pm 2.4\%$, which implies that the overall porosity is mainly affected by the initial dope concentration and not by the resulting membrane morphology. In addition, the degree of crystallinity was initially expected to have positive effect on mechanical properties. However, as the crystallinity increased from 57–69%, the respective

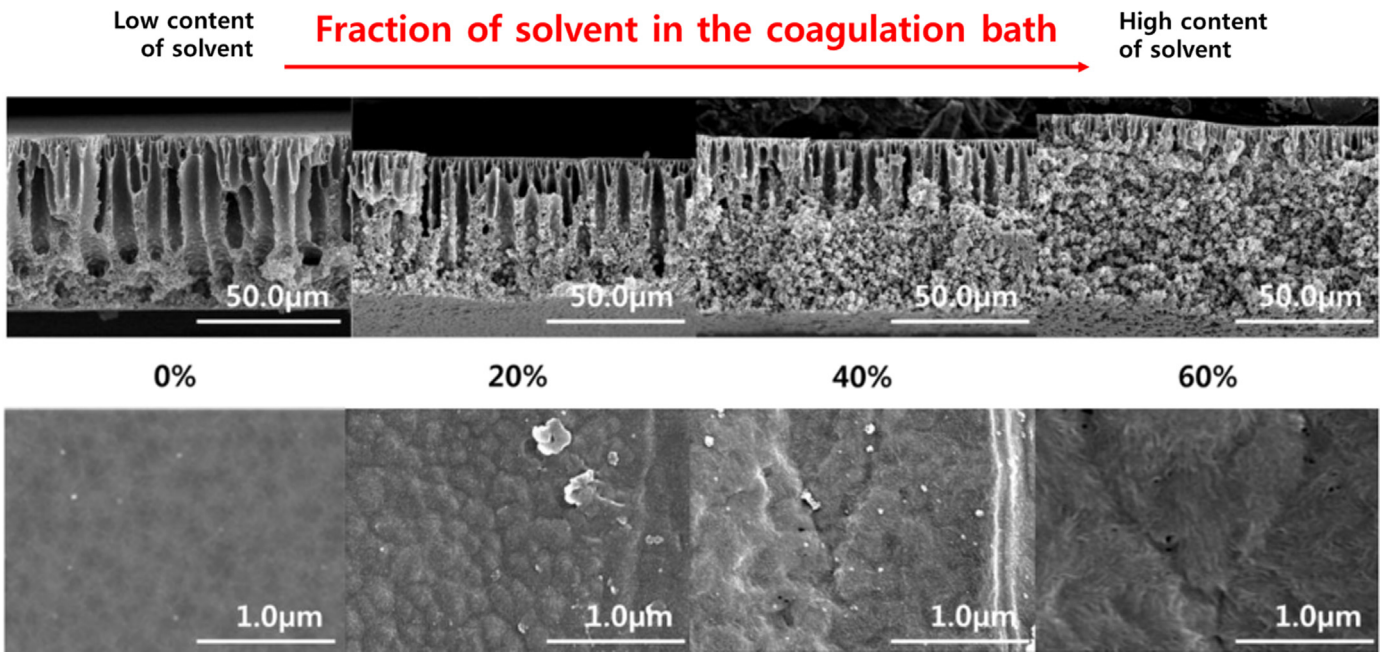

Fig. 4. Effect of the PolarClean® fraction in the coagulation bath on 15 wt% PVDF/ PolarClean® membranes at 5 °C.

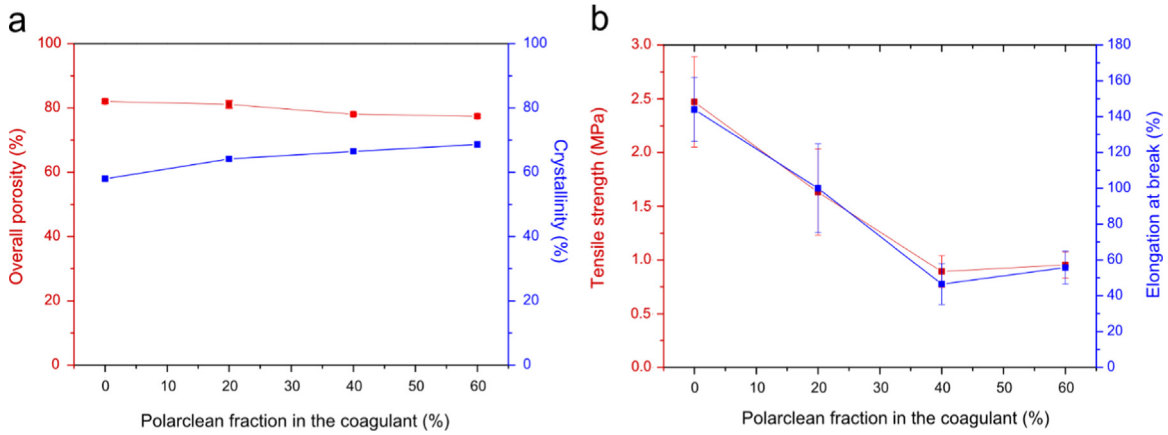

Fig. 5. The effects of the coagulation bath concentration on the PVDF/PolarClean® membranes: (a) overall porosity and crystallinity, and (b) tensile strength and elongation at break.

mechanical properties rather diminished supporting that the spherulitic TIPS morphology are unfavorable from the mechanical properties point of view.

3.3. *Effect of the concentration and temperature on PVDF/PolarClean® membranes*

When preparing polymeric membranes, water is almost universally used as the coagulation media due to its availability and low cost. As discussed in previous sections, PolarClean® has a high miscibility with water and hence, the NIPS effect is unavoidable during the membrane fabrication process. The NIPS effect can be controlled by changing the coagulation bath but it is not feasible on the large scale as a significant amount of solvent is required. A more practical and widely practiced method is to control the polymer concentration [47] and coagulation temperature [50], and to employ additives [50–52].

Fig. 6 exhibits the effects of the polymer concentration and coagulation bath temperature on the final membrane morphology. Several interesting trends are clear from the data. In order to interpret the observed morphology transformation, a detailed understanding of the membrane formation mechanism is necessary. In general, a NIPS process generates a dense skin and porous sub-layer. The dense surface is formed due to the solidification of the polymer top layer induced by a fast solvent outflow, and the porous sub-layer is induced from the liquid-liquid demixing where the solution phase separates into a polymer lean phase and a polymer rich phase [53,54]. The fast solvent outflow from the membrane top surface occurs as soon as a cast membrane comes in contact with a coagulation bath and hence, a dense skin is generally unavoidable during the NIPS process. On the other hand, the porous sub-layer morphology is governed by the solvent-nonsolvent diffusion rate and also by the solidification rate [43].

If the solvent-nonsolvent mutual diffusion rate is high, instantaneous demixing occurs with the formation of a macrovoid structure and if the mutual diffusion rate is low enough to go through delayed demixing, a bicontinuous structure is observed [34,55].

It can be seen in Fig. 6 that macrovoids progressively disappear with increasing polymer concentration and increasing coagulation bath temperature (T_{CB}). The effect of a higher polymer concentration is often observed. In this case, a higher polymer

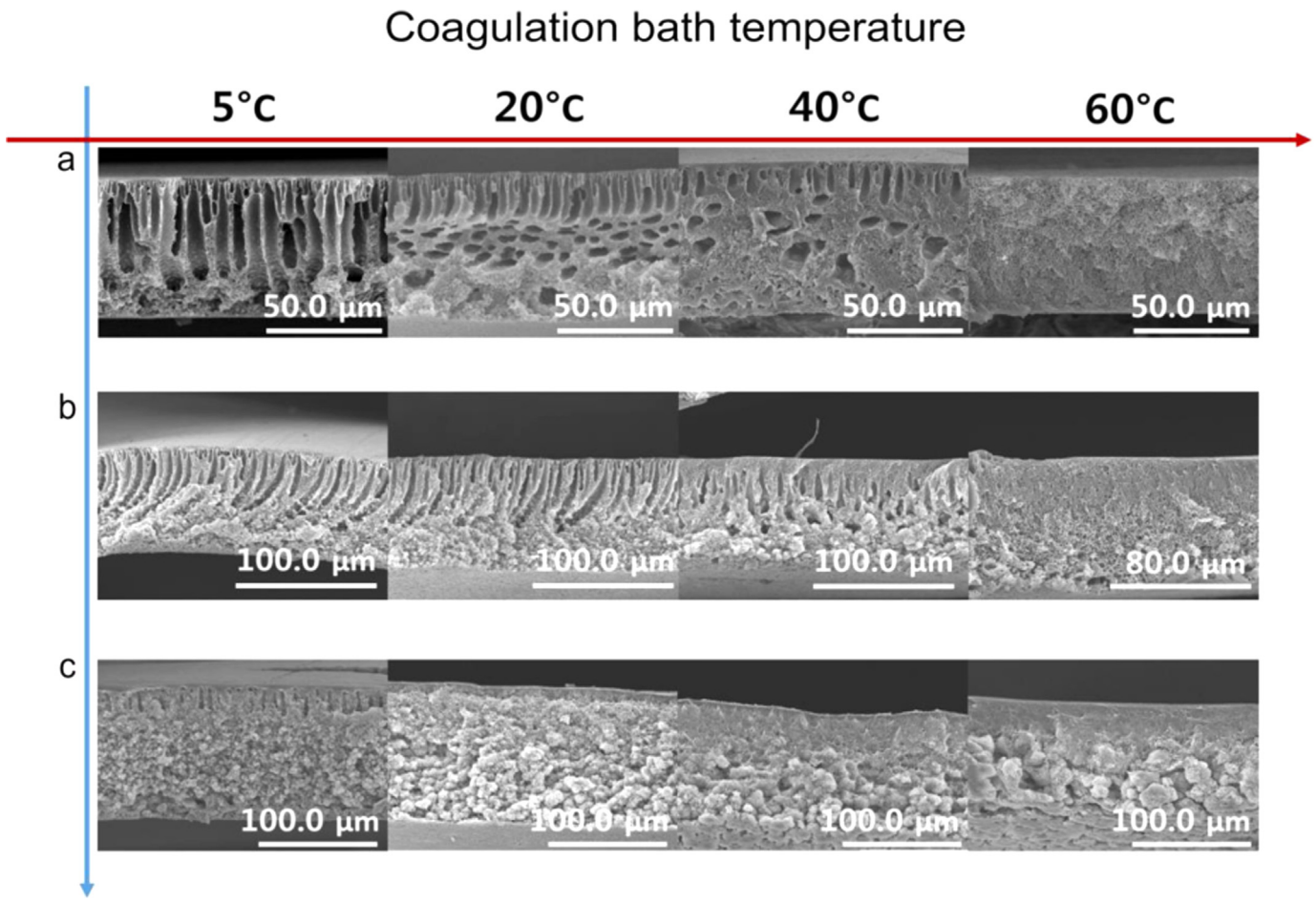

Fig. 6. The morphologies of membranes prepared with PolarClean® under different coagulation temperatures and polymer concentrations of (a) 15 wt%, (b) 20 wt%, and (c) 25 wt%.

concentration increases the solution viscosity which lowers the mutual diffusion and in turn, causes delayed demixing. Moreover, when the polymer concentration increases, especially for 25 wt% polymer membranes, approximately two thirds of the membrane cross-section showed a TIPS morphology (spherulites), indicating that the phase separation occurred primarily via the TIPS route. Such a result was expected from the phase diagram shown in Fig. 2, where the crystallization temperature (T_c) is 22 °C. In addition, as expected, the size of the spherulites increased with increasing T_{CB} as the spherulites have more time to grow [56].

While the high polymer concentration expectedly dampened the macrovoid structure, a high T_{CB} also induced the transition of the macrovoid structure into a bicontinuous structure, which is opposite to the widely accepted bicontinuous structure formation theory [55]. It is known that the bicontinuous structure results from spinodal decomposition and delayed demixing is considered as one of the ways to achieve a bicontinuous structure [24]. However, spinodal decomposition via fast penetration through the binodal region has been reported to also yield a bicontinuous morphology [57,58]. Understandably, this phenomenon is observed when the intrinsic mutual diffusion is very fast, which is the case with a higher T_{CB}.

To confirm this hypothesis, membranes were prepared at different coagulation temperatures with 15 wt% PVDF in NMP, as the characteristics of NMP are very similar to those of PolarClean® when it comes to membrane preparation via phase inversion. The resulting membrane structures also showed a transition from a finger-like structure into a bicontinuous structure, demonstrating the same trend observed in membranes prepared with PolarClean® (See Supporting information).

Fig. 7 summarizes the membrane characterization data for the membranes shown in Fig. 6. As expected, the disappearance of macrovoids is strongly correlated with a clear increase of the tensile strength. Particularly, the tensile strength of the 20 wt% membrane increased 3-fold from 2 MPa to 6 MPa. Such a drastic improvement may be attributed to the disappearance of macrovoids but also to the formation of a bicontinuous morphology with a well-connected membrane matrix [48]. On the other hand, there was no clear correlation between the T_{CB} and respective membrane elongation at break values (Fig. 7b).

Interestingly, the tensile strength of the 25 wt% polymer membrane also showed an increasing trend with increasing T_{CB}. Such a trend was unexpected as large spherulites formed at a higher T_{CB} and large spherulites have been shown to adversely affect the mechanical properties of membranes [56]. However, this argument is only appropriate if membranes are prepared employing only the TIPS process. As the membranes in this study were fabricated by the N-TIPS method, the NIPS effect must also be taken into account. As mentioned above, the nonsolvent penetration thickness is dependent on the temperature. Therefore, a high mutual diffusion rate is also expected in 25 wt% polymer membranes with the high T_{CB} environment, promoting more of a NIPS effect. However, compared to the lower polymer concentration (15 wt%), the higher polymer concentration (25 wt%) yields higher viscosity solutions which prevents nonsolvent penetration, resulting in the formation of a dense structure [34]. It can be seen clearly in Fig. 6 that the densified region on the top

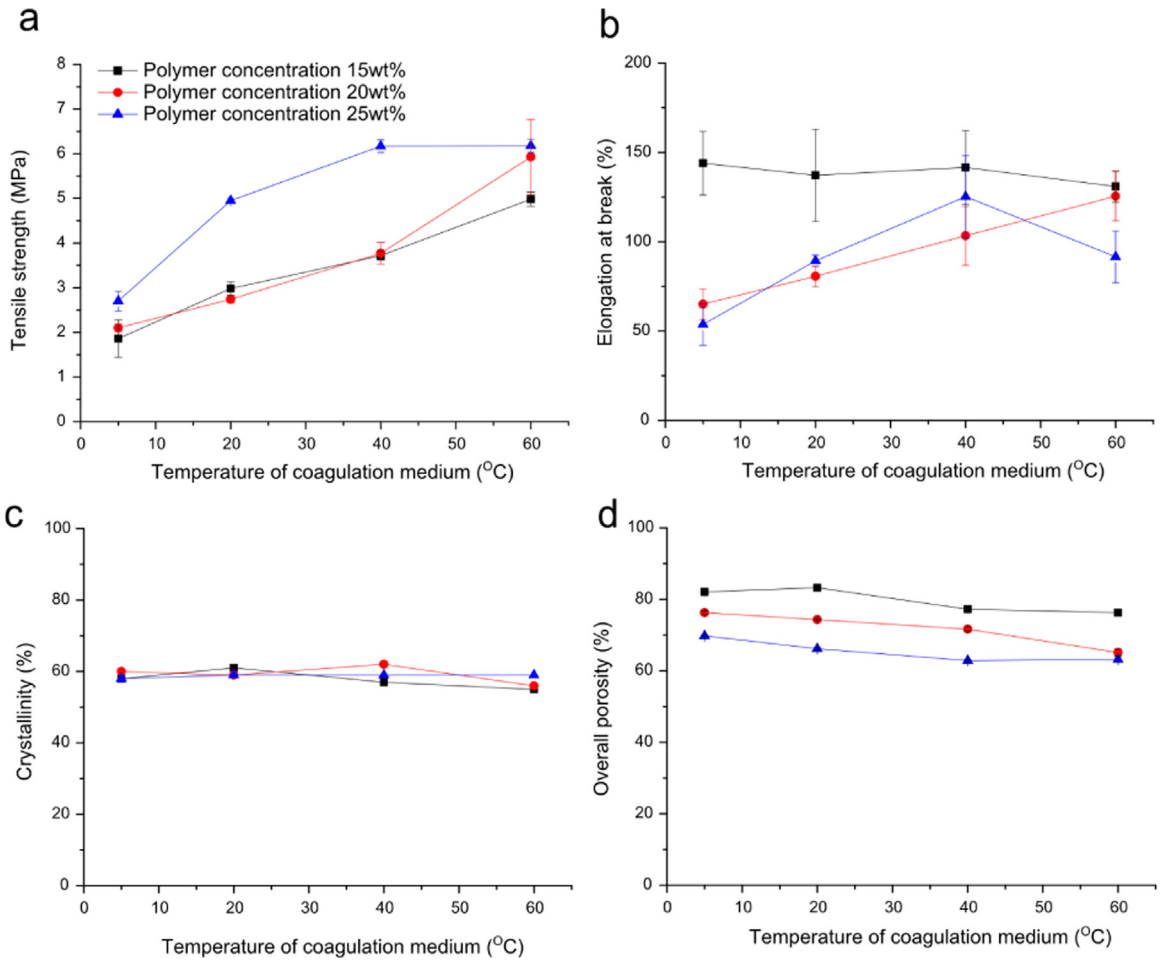

Fig. 7. PVDF/PolarClean® membrane characterization data for different coagulation temperatures: (a) tensile strength, (b) elongation at break, (c) crystallinity, and (d) overall porosity.

side of the 25 wt% membrane increased from 0.4–35% with a higher T_{CB}.

Notably, it can be seen in Fig. 7c that the crystallinity of the membranes were relatively similar, indicating that the differences of the mechanical properties are not due to the polymer crystallinity but to the macroscopic morphology. Also, the overall membrane porosity (Fig. 7d) decreased with increasing membrane polymer content but was not significantly affected by T_{CB}, again confirming that the final membrane porosity is mainly affected by the initial dope composition.

3.4. Morphology control in PVDF/PolarClean® membranes with additives

As shown in Figs. 4–7, varying the coagulation bath concentration, bath temperature, and polymer concentration all affected the membrane morphology and mechanical properties significantly but did not noticeably affect the overall porosity and crystallinity. Also, importantly, controlling the aforementioned parameters did not induce surface pores, resulting in a very low or no water permeability. Such a dense skin layer is an inevitable outcome from the high PolarClean® affinity towards water, resulting in a thin solidified layer during immersion precipitation. As the main objective of this work was to fabricate microporous membranes using an environmental friendly solvent and one of the effective ways to generate surface pores is to employ pore-forming additives [50–52], we evaluated three different sets of additives in this study: Pluronics F-127, PVP 10k, and LiCl & glycerol, in an attempt to fabricate microporous membranes. The Pluronics F-127 additive is gaining wide interest among membrane researchers with its excellent pore forming ability and unique amphiphilic properties [59]. Hassankiadeh et al., [29] investigated the effects of various additives on PVDF/PolarClean® hollow fiber membranes and concluded that PVP showed the highest performance improvement. Lee et al. [52] employed a mixture of LiCl and glycerol in PVDF/GBL hollow fiber membranes which showed a significant flux enhancement with a slight decline of the mechanical properties. For all of the prepared membranes with additives, the polymer concentration was fixed at 15 wt% as it exhibited the highest porosity with mechanical properties comparable to the 20 wt% membranes. A screening study was first conducted on the three sets of additives, as shown in Figs. 8 and 9.

The surface and cross-sectional SEM images in Fig. 8 clearly reveal that the addition of additives induces surface pores and the formation of macrovoids. Such phenomenon is well documented in the membrane literature, where additives move the initial dope composition closer to the binodal line, inducing instantaneous demixing to yield macrovoids. Simultaneously, as the additives themselves also have a reasonable affinity towards water, they also mix with water upon immersion, forming surface pores at the top surface.

The formation of macrovoids, as expected, weakened the membranes significantly. As shown in Fig. 9a, the tensile strength of the membranes with Pluronic F-127 and PVP 10K fell significantly from 5.1 MPa to 1.7 MPa. On the other hand, the addition of glycerol+LiCl did not induce macrovoids as much and hence,

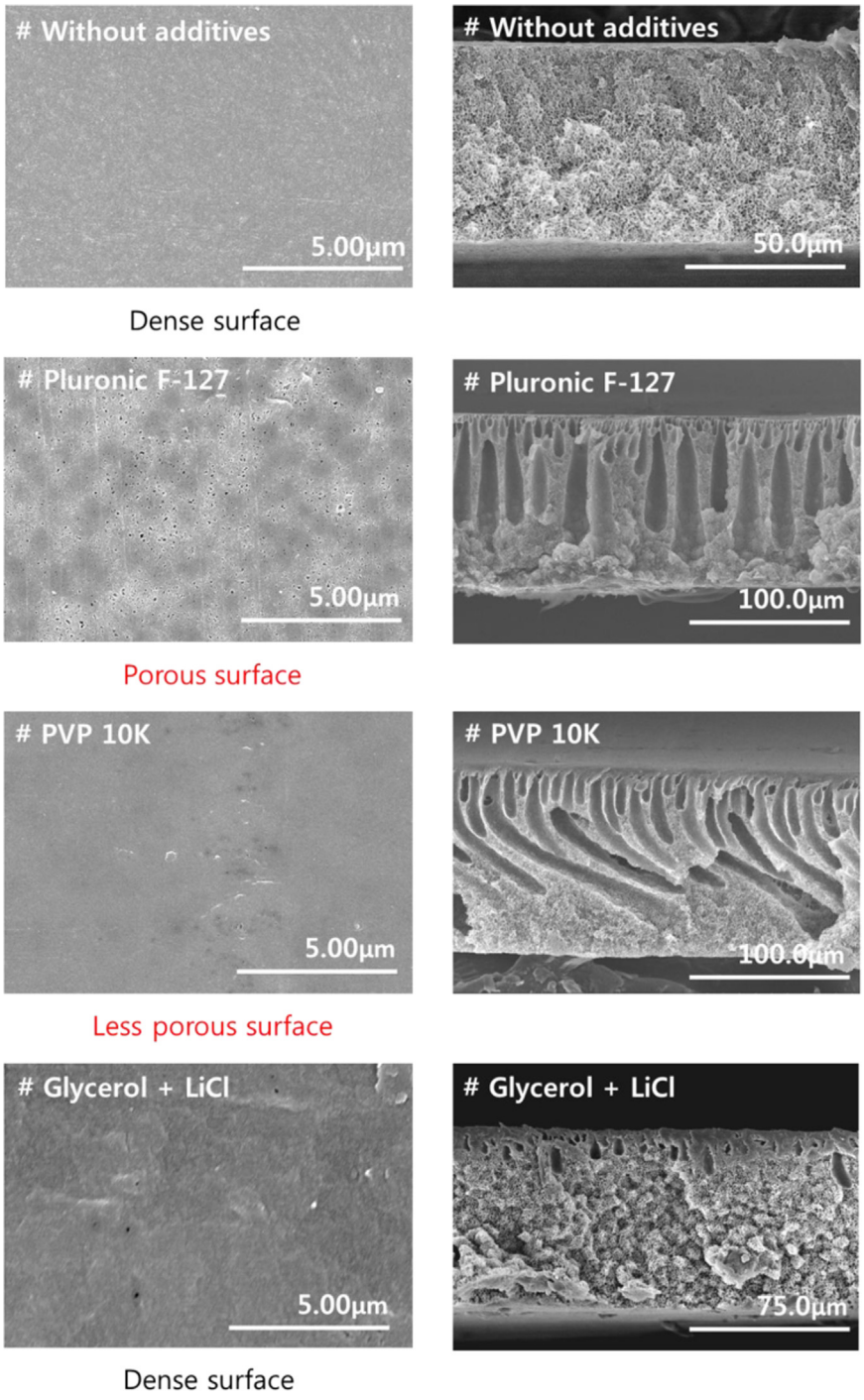

Fig. 8. The surface and cross-sectional morphologies of the membranes prepared with PolarClean® at 60 °C employing different additives.

the decrease of the tensile strength was lower (3.18 MPa). The elongation at break values also decreased with additives, confirming that the existence of macrovoids certainly deteriorates the mechanical properties.

Interestingly, although all of the membranes prepared with additives showed a macrovoid structure, there was a clear difference of the surface porosity between the employed additives. Among the additives, it can be seen in Fig. 9 that Pluronic F-127 induced the highest surface porosity and overall porosity. Pluronic F-127 is a type of poloxamer which is an amphiphilic copolymer of hydrophobic propylene oxide and hydrophilic ethylene oxide functional groups. When the prepared membranes were characterized using ATR-FTIR for residual additives, it was determined that Pluronic F-127 was completely removed from the PVDF matrix (see Supporting information). On the other hand, approximately 10% of the PVP10k (relative to the initial amount) remained in the PVDF membranes (see Supporting information). Previous studies have shown similar results where the PVP additive remained in the PVDF membranes and different chemical treatments (*e.g.* NaOCl) were not effective in removing the residual PVP [29]. It is now well accepted that PVP has a high affinity with PVDF polymer and the two polymers physically intertwine together in solution. In this respect, the use of the PVP additive is one of the effective hydrophilic modification techniques of fluoropolymers, but not an effective pore former as it tends to intertwine with PVDF [60]. On the contrary, it has been reported that the high

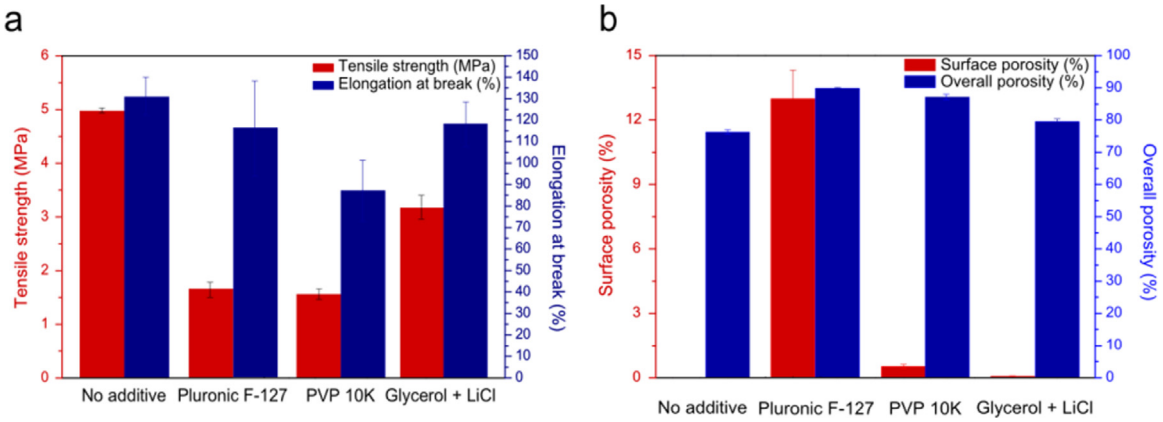

Fig. 9. Membrane characterization data at 60 °C: (a) tensile strength and elongation at break, and (b) surface porosity and overall porosity.

micelle forming ability and the aggregation behavior of Pluronic F-127 helps to induce surface pores [61,62]. Hence, it can be deduced that Pluronic F-127 is a more effective pore former as it does not intertwine with PVDF like PVP and hence, is more easily removed from the membrane.

Further performance optimization was carried out using Pluronic F-127 by varying the additive concentration (5 and 10 wt%) and coagulation bath temperature (20, 40, and 60 °C).

First, it can be seen in Fig. 10a and b that no significant trends of the mechanical properties of the membranes were observed when varying the Pluronic concentration and coagulation bath temperature (T_{CB}). Although a higher T_{CB} was found to suppress the macrovoids, as presented in Section 3.4, this effect was not observed when additives were used. Secondly, there were no noticeable trends of the membrane elongation properties with respect to the Pluronic content and T_{CB}. Interestingly, the overall porosity of the membranes increased from 76.27–89.9% with the addition of Pluronic. However, there was no relationship between the Pluronic content (5 or 10 wt%) and the overall porosity.

On the other hand, employing Pluronic F-127 additives certainly improved the membrane water flux, as shown in Fig. 10d. More specifically, clear increasing trends of the water flux with increasing bath temperature (T_{CB}) and Pluronic content were observed, with the water flux reaching as high as 2700 L m^{-2} h^{-1} bar^{-1}. It should be stressed that the initial water flux reached up to 6000 L m^{-2} h^{-1} bar^{-1} but the value dropped approximately 60% on average after 5 h of compaction (See Supporting information).

The SEM images shown in Fig. 11 support the observed flux data in which a higher coagulation bath temperature (T_{CB}) drastically increased the surface porosity and pore size. With increasing T_{CB}, the surface porosity increased from 2.4% to 12.7% and the corresponding mean pore size also increased from 23 nm to 41 nm (5 wt% Pluronic). This trend may be attributed to the faster diffusion rate of the additive into the coagulation bath (water), forming more and larger pores.

On the other hand, Pluronic concentration did not show distinct effect on the surface porosity nor the pore size. For instance, the measured surface porosity data for 5 wt% and 10 wt% Pluronic overlapped at the same T_{CB}, within the error range (Fig. 11e). In addition, the pore size distribution analysis indicates that the mean pore size increased with increasing T_{CB} but no clear trend could be deduced with Pluronic concentration (see Supporting information for the full distribution data). It is speculated that above a certain Pluronic concentration, there is no additional effect on the surface porosity and mean pore size of the membranes.

In general, the membranes prepared *via* NIPS exhibit an asymmetric morphology with a gradient of the pore size along the membrane depth, showing a wide log-normal pore size distribution. On the other hand, membranes prepared *via* TIPS typically show a very narrow pore size distribution. In this work, the membranes prepared *via* the N-TIPS method showed log-normal pore size distribution (see Supporting information) and the distribution tended to become wider with increasing T_{CB}.

It is known that the water permeability in MF/UF membranes is determined by the surface porosity and mean pore size of the membrane. [24] Comparing the overall porosity and surface porosity data with respective permeability data (Fig. 10c and d), it can be seen that the membrane permeability is mainly affected by the surface porosity rather than the overall porosity.

Fig. 12 compares the performance of the PVDF/PolarClean® membranes produced in this work to the current TIPS PVDF upperbound. It can be seen that the membrane performance is competitive, close to the current upper bound. It is expected that further improvements can be achieved *via* hydrophilic modification of the membranes. It should be stressed that the membranes in this work were prepared using an environmental friendly PolarClean® solvent, confirming that MF and UF membranes can be fabricated using greener alternatives. Additionally, the prepared membranes showed an extremely high overall porosity, reaching up to 90%, indicating their high potential for membrane distillation applications.

4. Conclusion

In this study, we fabricated microporous PVDF membranes using an environmental friendly PolarClean® solvent *via* the N-TIPS method. PolarClean® is a water-soluble solvent which is highly biodegradable and non-toxic. It was found that the high affinity of PolarClean® towards the coagulation media induced a NIPS effect during the TIPS process, resulting in an unusual N-TIPS morphology. This interesting phenomenon was studied in detail from thermodynamic and kinetic perspectives, and feasible explanations to the observed morphology were suggested. The effects of the polymer concentration, coagulation bath composition, and bath temperature on the final membrane morphology and respective properties were investigated. In order to form surface pores, three different sets of additives (Pluronic F-127, PVP10k, and LiCl & glycerol) were screened and Pluronic F-127 was found to be the most effective pore-former. The pore-forming additives drastically improved the water permeability at the expense of the mechanical properties. Also, it was shown that the surface pore size and distribution can be controlled by varying the bath temperature and additive content. The membranes produced in this work demonstrated competitive performance compared to

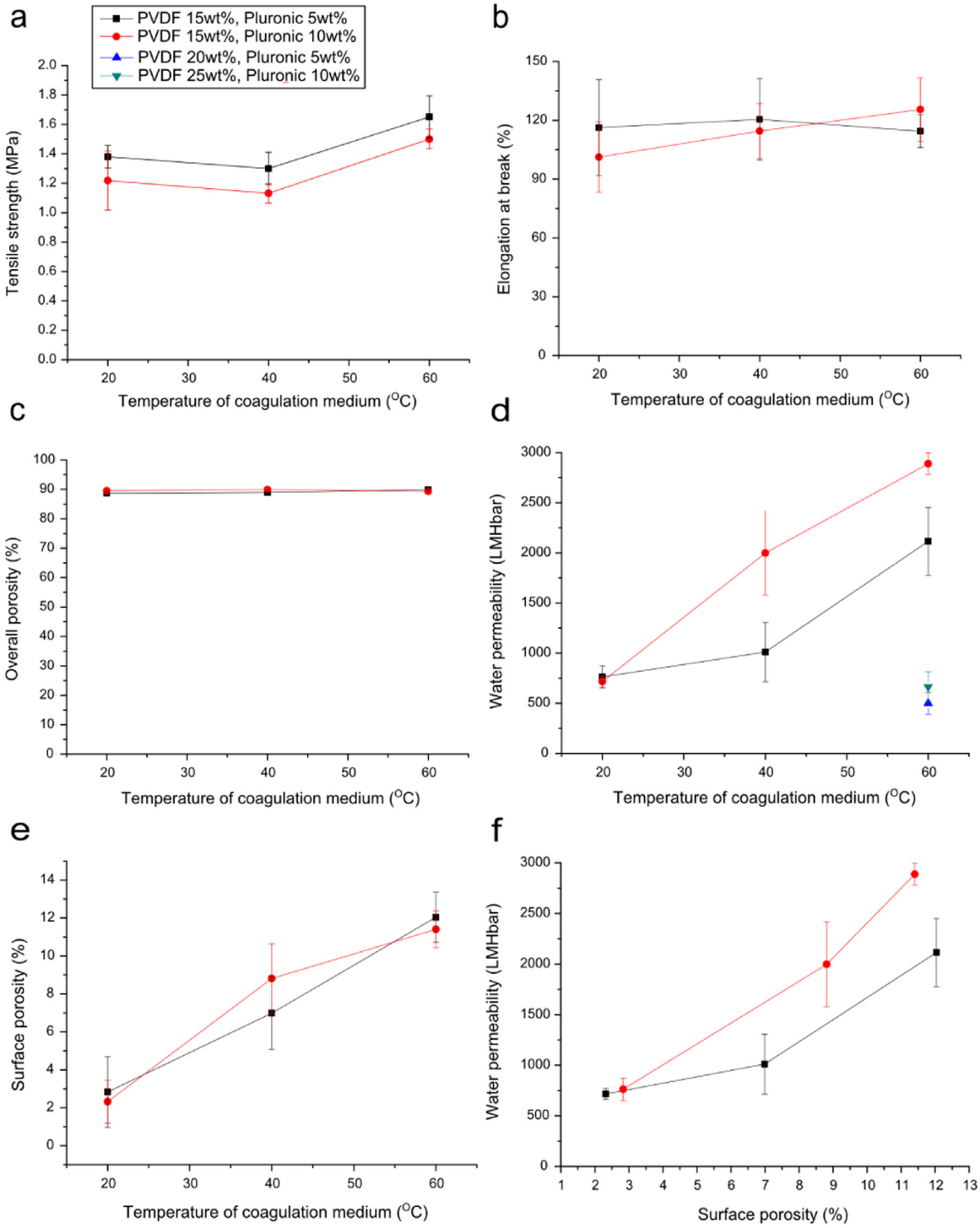

Fig. 10. Characterization data of the membranes prepared with Pluronic F-127 additives at different coagulation temperatures: (a) tensile strength, (b) elongation at break, (c) overall porosity, (d) water permeability, (e) surface porosity, and (f) water permeability as a function of the surface porosity.

membranes reported in the literature and it is envisaged that the proposed PolarClean® solvent offers a more sustainable and green alternative to fabricate microporous PVDF membranes.

Acknowledgements

We would like to acknowledge the financial support of Solvay Specialty Polymers and the Nano-Material Technology Development Program through the National Research Foundation of Korea (NRF) funded by the Ministry of ICT, Science and Technology of Korea (2012M3A7B4049745).

Appendix A. Supporting information

Supplementary data associated with this article can be found in the online version at http://dx.doi.org/10.1016/j.memsci.2016.04.069.

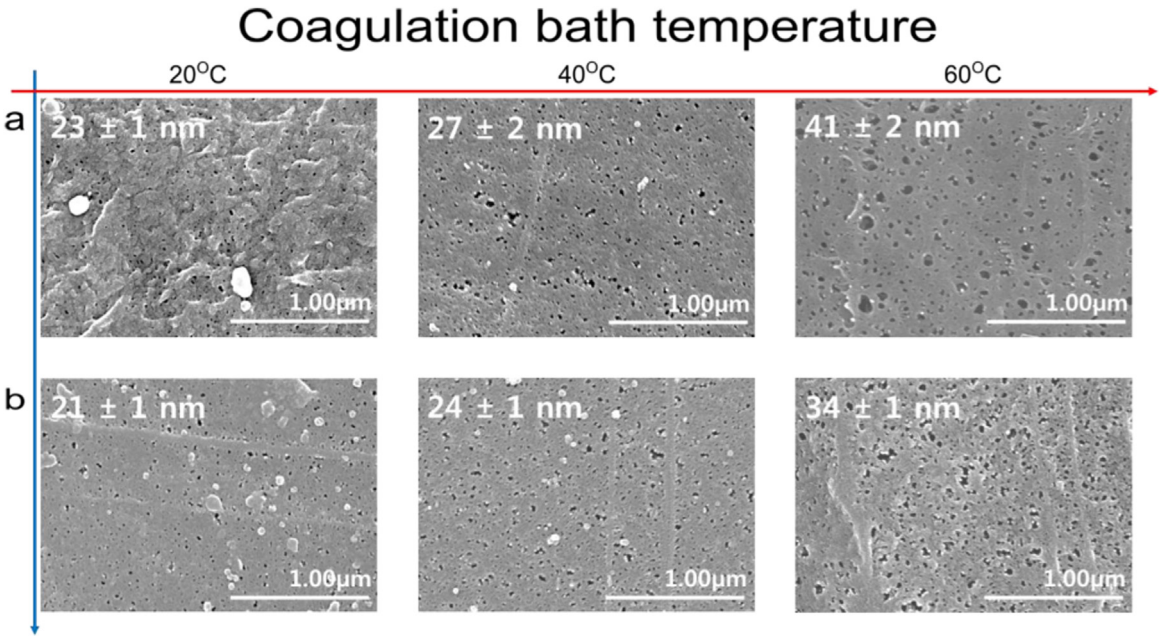

Fig. 11. Surface SEM images of membranes prepared with the Pluronic F-127 additive. The numbers in the images refer to the mean pore size of the membranes for additive concentrations of (a) 5 wt% and (b) 10 wt%.

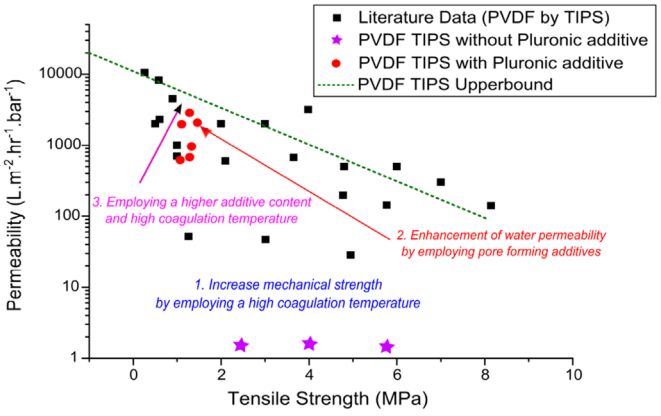

Fig. 12. Performance comparison of the membranes fabricated in this study to other reported PVDF membranes using the upper bound from a recent TIPS review [12].

References

[1] Z. Cui, N.T. Hassankiadeh, Y. Zhuang, E. Drioli, Y.M. Lee, Crystalline polymorphism in poly (vinylidenefluoride) membranes, Prog. Polym. Sci. 51 (2015) 94–126.

[2] A. Basile, A. Cassano, N.K. Rastogi, Advances in Membrane Technologies for Water Treatment: Materials, Processes and Applications, Elsevier, Amsterdam, 2015.

[3] W. Li, G.-Q. Ling, P. Huang, K. Li, H.-Q. Lu, F.-X. Hang, Y. Zhang, C.-F. Xie, D.-J. Lu, H. Li, Performance of ceramic microfiltration membranes for treating carbonated and filtered remelt syrup in sugar refinery, J. Food Eng. 170 (2016) 41–49.

[4] B. Chakravorty, A. Layson, Ideal feed pretreatment for reverse osmosis by continuous microfiltration, Desalination 110 (1997) 143–149.

[5] E. Curcio, E. Drioli, Membrane distillation and related operations—a review, Sep. Purif. Rev. 34 (2005) 35–86.

[6] J.H. Kim, S.H. Park, M. Lee, S.M. Lee, W.H. Lee, K.H. Lee, N.R. Kang, H.J. Jo, J. F. Kim, E. Drioli, Thermally Rearranged Polymer Membranes for Desalination, Energy Environ. Sci. 9 (2016) 878–884.

[7] Z. Cui, E. Drioli, Y.M. Lee, Recent progress in fluoropolymers for membranes, Prog. Polym. Sci. 39 (2014) 164–198.

[8] G.R. Guillen, Y. Pan, M. Li, E.M. Hoek, Preparation and characterization of membranes formed by nonsolvent induced phase separation: a review, Ind. Eng. Chem. Res. 50 (2011) 3798–3817.

[9] M. Yeow, Y. Liu, K. Li, Morphological study of poly (vinylidene fluoride) asymmetric membranes: effects of the solvent, additive, and dope temperature, J. Appl. Polym. Sci. 92 (2004) 1782–1789.

[10] D.R. Lloyd, K.E. Kinzer, H. Tseng, Microporous membrane formation via thermally induced phase separation. I. Solid-liquid phase separation, J. Membr. Sci. 52 (1990) 239–261.

[11] M. Gu, J. Zhang, X. Wang, H. Tao, L. Ge, Formation of poly (vinylidene fluoride PVDF membranes via thermally induced phase separation, Desalination 192 (2006) 160–167.

[12] J.F. Kim, J.H. Kim, Y.M. Lee, E. Drioli, Thermally induced phase separation and electrospinning methods for emerging membrane applications: a review, AIChE J. 62 (2015) 461–490.

[13] A. Figoli, T. Marino, S. Simone, E. Di Nicolo, X.-M. Li, T. He, S. Tornaghi, E. Drioli, Towards non-toxic solvents for membrane preparation: a review, Green Chem. 16 (2014) 4034–4059.

[14] M. Razali, J.F. Kim, M. Attfield, P.M. Budd, E. Drioli, Y.M. Lee, G. Szekely, Sustainable wastewater treatment and recycling in membrane manufacturing, Green Chem. 17 (2015) 5196–5205.

[15] M. Reisch, Solvent users look to replace NMP, Chem. Eng. News 86 (2008) 32.

[16] U. Heudorf, V. Mersch-Sundermann, J. Angerer, Phthalates: toxicology and exposure, Int. J. Hyg. Environ. Health 210 (2007) 623–634.

[17] M. Becker, S. Edwards, R.I. Massey, Toxic chemicals in toys and children's products: limitations of current responses and recommendations for government and industry, Environ. Sci. Technol. 44 (2010) 7986–7991.

[18] B.J. Cha, J.M. Yang, Preparation of poly (vinylidene fluoride) hollow fiber membranes for microfiltration using modified TIPS process, J. Membr. Sci. 291 (2007) 191–198.

[19] S. Rajabzadeh, T. Maruyama, T. Sotani, H. Matsuyama, Preparation of PVDF hollow fiber membrane from a ternary polymer/solvent/nonsolvent system via thermally induced phase separation (TIPS) method, Sep. Purif. Technol. 63 (2008) 415–423.

[20] S. Rajabzadeh, T. Maruyama, Y. Ohmukai, T. Sotani, H. Matsuyama, Preparation of PVDF/PMMA blend hollow fiber membrane via thermally induced phase separation (TIPS) method, Sep. Purif. Technol. 66 (2009) 76–83.

[21] S.-I. Sawada, C. Ursino, F. Galiano, S. Simone, E. Drioli, A. Figoli, Effect of citrate-based non-toxic solvents on poly (vinylidene fluoride) membrane preparation via thermally induced phase separation, J. Membr. Sci. 493 (2015) 232–242.

[22] J.F. Kim, J.T. Jung, H.H. Wang, S.Y. Lee, T. Moore, A. Sanguineti, E. Drioli, Y. M. Lee, Microporous PVDF membranes via thermally induced phase separation (TIPS) and stretching methods, J. Membr. Sci. 509 (2016) 94–104.

[23] Z. Cui, N.T. Hassankiadeh, S.Y. Lee, K.T. Woo, J.M. Lee, A. Sanguineti, V. Arcella, Y.M. Lee, E. Drioli, Tailoring novel fibrillar morphologies in poly (vinylidene fluoride) (membranes using a low toxic triethylene glycol diacetate (TEGD)A) diluent, J. Membr. Sci. 473 (2015) 128–136.

[24] M. Mulder, Basic Principles of Membrane Technology, Springer Science & Business Media, Dordrecht, 1996.

[25] S. Deshmukh, K. Li, Effect of ethanol composition in water coagulation bath on morphology of PVDF hollow fibre membranes, J. Membr. Sci. 150 (1998) 75–85.

[26] H. Matsuyama, Y. Takida, T. Maki, M. Teramoto, Preparation of porous membrane by combined use of thermally induced phase separation and immersion precipitation, Polymer 43 (2002) 5243–5248.

[27] X. Li, Y. Wang, X. Lu, C. Xiao, Morphology changes of polyvinylidene fluoride membrane under different phase separation mechanisms, J. Membr. Sci. 320 (2008) 477–482.

[28] T.T. Jin, Z.P. Zhao, K.C. Chen, Preparation of a poly (vinyl chloride) ultrafiltration membrane through the combination of thermally induced phase separation and non-solvent-induced phase separation, J. Appl. Polym. Sci. 133 (2016).
[29] N.T. Hassankiadeh, Z. Cui, J.H. Kim, D.W. Shin, S.Y. Lee, A. Sanguineti, V. Arcella, Y.M. Lee, E. Drioli, Microporous poly (vinylidene fluoride) hollow fiber membranes fabricated with PolarClean as water-soluble green diluent and additives, J. Membr. Sci. 479 (2015) 204–212.
[30] T.-H. Young, L.-P. Cheng, D.-J. Lin, L. Fane, W.-Y. Chuang, Mechanisms of PVDF membrane formation by immersion-precipitation in soft (1-octanol) and harsh (water) nonsolvents, Polymer 40 (1999) 5315–5323.
[31] L.-P. Cheng, T.-H. Young, L. Fang, J.-J. Gau, Formation of particulate microporous poly (vinylidene fluoride) membranes by isothermal immersion precipitation from the 1-octanol/dimethylformamide/poly (vinylidene fluoride) system, Polymer 40 (1999) 2395–2403.
[32] P. Van de Witte, P. Dijkstra, J. Van den Berg, J. Feijen, Phase separation processes in polymer solutions in relation to membrane formation, J. Membr. Sci. 117 (1996) 1–31.
[33] S.K. Yong, J.K. Hyo, Y.K. Un, Asymmetric membrane formation via immersion precipitation method. I. Kinetic effect, J. Membr. Sci. 60 (1991) 219–232.
[34] H. Strathmann, K. Kock, P. Amar, R. Baker, The formation mechanism of asymmetric membranes, Desalination 16 (1975) 179–203.
[35] A. Bottino, G. Capannelli, S. Munari, A. Turturro, Solubility parameters of poly (vinylidene fluoride), J. Polym. Sci., Part B: Polym. Phys. 26 (1988) 785–794.
[36] D.-J. Lin, C.-L. Chang, T.-C. Chen, L.-P. Cheng, On the Structure of porous Poly (vinylidene Fluoride) membrane prepared by phase inversion from Water-NMP-PVDF system, Tamkang. J. Sci. Eng. 5 (2002) 95–98.
[37] J. Brandrup, E.H. Immergut, E.A. Grulke, A. Abe, D.R. Bloch, Polymer Handbook, Wiley, New York, 1999.
[38] C.M. Hansen, Hansen Solubility Parameters: A User's Handbook, CRC Press, London, 2007.
[39] Y.K. Ong, N. Widjojo, T.-S. Chung, Fundamentals of semi-crystalline poly (vinylidene fluoride) membrane formation and its prospects for biofuel (ethanol and acetone) separation via pervaporation, J. Membr. Sci. 378 (2011) 149–162.
[40] G.-L. Ji, B.-K. Zhu, Z.-Y. Cui, C.-F. Zhang, Y.-Y. Xu, PVDF porous matrix with controlled microstructure prepared by TIPS process as polymer electrolyte for lithium ion battery, Polymer 48 (2007) 6415–6425.
[41] Y. Su, C. Chen, Y. Li, J. Li, Preparation of PVDF membranes via TIPS method: The effect of mixed diluents on membrane structure and mechanical property, J. Macromol. Sci., Pure Appl. Chem. 44 (2007) 305–313.
[42] G.L. Ji, C.H. Du, B.K. Zhu, Y.Y. Xu, Preparation of porous PVDF membrane via thermally induced phase separation with diluent mixture of DBP and DEHP, J. Appl. Polym. Sci. 105 (2007) 1496–1502.
[43] S.A. McKelvey, W.J. Koros, Phase separation, vitrification, and the manifestation of macrovoids in polymeric asymmetric membranes, J. Membr. Sci. 112 (1996) 29–39.
[44] L. Yu, F. Yang, M. Xiang, Phase separation in a PSf/DMF/water system: a proposed mechanism for macrovoid formation, RSC Adv. 4 (2014) 42391–42402.
[45] Y. Doi, H. Matsumura, Chemical resistant filters, U.S. Patent No. 5022990, 1991.
[46] M. Di Luccio, R. Nobrega, C. Borges, Microporous anisotropic phase inversion membranes from bisphenol-A polycarbonate: study of a ternary system, Polymer 41 (2000) 4309–4315.
[47] Y.S. Nam, T.G. Park, Biodegradable polymeric microcellular foams by modified thermally induced phase separation method, Biomaterials 20 (1999) 1783–1790.
[48] W. Ma, J. Zhang, B.Vd Bruggen, X. Wang, Formation of an interconnected lamellar structure in PVDF membranes with nanoparticles addition via solid-liquid thermally induced phase separation, J. Appl. Polym. Sci. 127 (2013) 2715–2723.
[49] Y. Lin, Y. Tang, H. Ma, J. Yang, Y. Tian, W. Ma, X. Wang, Formation of a bicontinuous structure membrane of polyvinylidene fluoride in diphenyl carbonate diluent via thermally induced phase separation, J. Appl. Polym. Sci. 114 (2009) 1523–1528.
[50] C.H. Loh, R. Wang, L. Shi, A.G. Fane, Fabrication of high performance polyethersulfone UF hollow fiber membranes using amphiphilic Pluronic block copolymers as pore-forming additives, J. Membr. Sci. 380 (2011) 114–123.
[51] S. Simone, A. Figoli, A. Criscuoli, M. Carnevale, A. Rosselli, E. Drioli, Preparation of hollow fibre membranes from PVDF/PVP blends and their application in VMD, J. Membr. Sci. 364 (2010) 219–232.
[52] J. Lee, B. Park, J. Kim, S.B. Park, Effect of PVP, lithium chloride, and glycerol additives on PVDF dual-layer hollow fiber membranes fabricated using simultaneous spinning of TIPS and NIPS, Macromol. Res. 23 (2015) 291–299.
[53] H. Bokhorst, F. Altena, C. Smolders, Formation of asymmetric cellulose acetate membranes, Desalination 38 (1981) 349–360.
[54] M. Mulder, J.O. Hendrikman, J. Wijmans, C. Smolders, A rationale for the preparation of asymmetric pervaporation membranes, J. Appl. Polym. Sci. 30 (1985) 2805–2820.
[55] C. Smolders, A. Reuvers, R. Boom, I. Wienk, Microstructures in phase-inversion membranes. Part 1. Formation of macrovoids, J. Membr. Sci. 73 (1992) 259–275.
[56] I. Wienk, R. Boom, M. Beerlage, A. Bulte, C. Smolders, H. Strathmann, Recent advances in the formation of phase inversion membranes made from amorphous or semi-crystalline polymers, J. Membr. Sci. 113 (1996) 361–371.
[57] R. Boom, I. Wienk, T. Van den Boomgaard, C. Smolders, Microstructures in phase inversion membranes. Part 2. The role of a polymeric additive, J. Membr. Sci. 73 (1992) 277–292.
[58] Y. Su, C. Kuo, D. Wang, J. Lai, A. Deratani, C. Pochat, D. Bouyer, Interplay of mass transfer, phase separation, and membrane morphology in vapor-induced phase separation, J. Membr. Sci. 338 (2009) 17–28.
[59] C.H. Loh, R. Wang, Effects of additives and coagulant temperature on fabrication of high performance PVDF/pluronic F127 blend hollow fiber membranes via nonsolvent induced phase separation, Chin. J. Chem. Eng. 20 (2012) 71–79.
[60] M. Nasir, H. Matsumoto, M. Minagawa, A. Tanioka, T. Danno, H. Horibe, Preparation of porous PVDF nanofiber from PVDF/PVP blend by electrospray deposition, Polym. J. 39 (2007) 1060–1064.
[61] W. Zhao, Y. Su, C. Li, Q. Shi, X. Ning, Z. Jiang, Fabrication of antifouling polyethersulfone ultrafiltration membranes using Pluronic F127 as both surface modifier and pore-forming agent, J. Membr. Sci. 318 (2008) 405–412.
[62] P. Alexandridis, J.F. Holzwarth, T.A. Hatton, Micellization of poly (ethylene oxide)-poly (propylene oxide)-poly (ethylene oxide) triblock copolymers in aqueous solutions: thermodynamics of copolymer association, Macromolecules 27 (1994) 2414–2425.